International Journal of Solids and Structures 51 (2014) 2327–2335

Contents lists available at ScienceDirect

International Journal of Solids and Structures

journal homepage: www.elsevier.com/locate/ijsolstr

On micromechanical-statistical modeling of microscopically damaged interfaces under antiplane deformations

Xue Wang *, Hui Fan, Whye-Teong Ang

Division of Engineering Mechanics, School of Mechanical and Aerospace Engineering, Nanyang Technological University, Singapore 639798, Singapore

ARTICLE INFO

Article history:
Received 18 December 2013
Received in revised form 21 February 2014
Available online 18 March 2014

Keywords:
Micromechanics
Microscopically damaged interface
Effective stiffness
Hypersingular integral equations

ABSTRACT

A microscopically damaged interface between two elastic half-spaces under anti-plane deformations is modeled using randomly distributed interfacial micro-cracks. The micro-crack length is a continuous random variable following a given probability distribution. The micromechanical-statistical model of the interface, formulated and solved in terms of hypersingular integral equations, is used to estimate the effective stiffness of the interface. The number of micro-cracks per period length of the interface required to homogenize the effective interface stiffness is examined. Also investigated are the effects of the micro-crack length and the crack-tip gap between two neighboring micro-cracks on the effective stiffness.

1. Introduction

Micro-roughness of surfaces (Hamidi et al., 2004) or thermally induced residual stresses during manufacturing processes (Nix, 1989) may give rise to microscopic voids and defects in the interface between two solids which are otherwise perfectly bonded. As illustrated in Fig. 1, for macro-scale analyses, a microscopically damaged interface between two solids may be modeled as a continuous distribution of springs characterized by stiffness parameters.

One of the earlier works dealing with imperfect spring-like interfaces is Jones and Whittier (1967). In Jones and Whittier (1967), the interaction of elastic waves with flexibly bonded interfaces is studied. Since then, many boundary value problems involving spring-like models of imperfect interfaces have been solved (see, for example, Ang, 2007; Fan and Wang, 2003; Margetan et al., 1988; Zhong and Meguid, 1997). Nevertheless, the micromechanical analysis of microscopically damaged interfaces, which includes estimating the effective properties of interfaces, has been investigated by relatively fewer researchers.

Micromechanical models based on continuum mechanics, such as the Voigt approximation, the Reuss approximation, the self-consistent scheme and the three-phase model, for estimating the effective material properties of microscopically heterogenous solids may be found in the research literature (Aboudi, 1991; Christensen, 1990; Li and Wang, 2008). Those models do not attempt to capture all the minute details of the microstructures in the heterogeneous solids. For a more realistic micro-mechanical analysis but one still based on continuum mechanics, the microstructures may be modeled as, for example, randomly generated holes or inclusions in the solids (see Elvin, 1996; Roberts and Garboczi, 1999; Torquato, 2002). Such an approach has been extended by Wang et al. (2012) to the micromechanical analysis of a microscopically damaged interface between two elastic half-spaces under antiplane deformations.

In Wang et al. (2012), the microscopically damaged plane interface is modeled using periodically distributed interfacial micro-cracks. A period length of the damaged interface contains an arbitrary number of randomly positioned micro-cracks. The length of a micro-crack is taken to be a continuous random variable following a given probability distribution. The procedure for estimating the effective stiffness of the interface, which requires solving numerically hypersingular integral equations for the micro-cracks, is described in detail in Wang et al. (2012). The hypersingular integral formulation is advantageous in the micromechanical analysis of the interface (Ang, 2013) as the jump in the displacement across opposite faces of each of the micro-cracks appears directly as an unknown function in the integral equations. Thus, no post-processing of the numerical solution of the integral equations is required to compute the interfacial displacement jump.

Nevertheless, only very limited statistical results for the effective stiffness of the interface are obtained and presented in Wang et al. (2012) using micro-cracks with normally distributed lengths. In reality, the length of a micro-crack may not vary according to a normal distribution. In the present paper, a more realistic

* Corresponding author. Tel.: +65 6790 4280.
E-mail address: XWANG20@e.ntu.edu.sg (X. Wang).

http://dx.doi.org/10.1016/j.ijsolstr.2014.03.001
0020-7683/

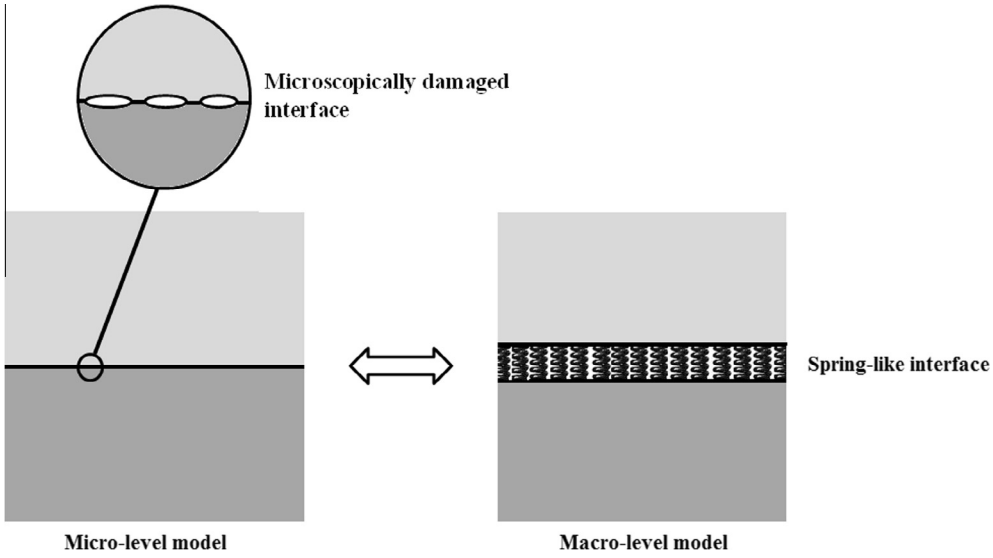

Fig. 1. Micro-level and macro-level models of the damaged interface.

statistical variation of the micro-crack length, based on the chi-squared (χ^2) distribution, is used to generate randomly the length of each micro-crack. The number of micro-cracks per period length of the interface required to homogenize the effective stiffness is examined. Also investigated are the effects of the micro-crack length and the crack-tip gap between two neighboring micro-cracks on the effective stiffness.

2. Micromechanical model

With reference to a Cartesian coordinate frame denoted by $Ox_1x_2x_3$, consider two dissimilar homogeneous anisotropic elastic half-spaces occupying the regions $x_2 > 0$ and $x_2 < 0$. The plane interface $x_2 = 0$ joining the half-spaces is microscopically damaged containing microscopic voids and defects.

The bimaterial undergoes an antiplane elastostatic deformation such that the only non-zero component of the displacement field is along x_3 direction. The elastic displacement $u_3(x_1, x_2)$ and stress $\sigma_{3i}(x_1, x_2)$ along the microscopic portion $0 < x_1 < l$ of the damaged interface may be homogenized by the averaging procedure

$$\begin{aligned}\overline{u}_3(\overline{x}_1, 0^{\pm}) &= \frac{1}{2l}\int_{\overline{x}_1-l}^{\overline{x}_1+l} u_3(x_1, 0^{\pm})dx_1,\\ \overline{\sigma}_{3i}(\overline{x}_1, 0^{\pm}) &= \frac{1}{2l}\int_{\overline{x}_1-l}^{\overline{x}_1+l} \sigma_{3i}(x_1, 0^{\pm})dx_1,\end{aligned} \tag{1}$$

where $\overline{x}_1$ denotes the midpoint of the microscopic portion of the interface.

In terms of the homogenized field variables $\overline{u}_3$ and $\overline{\sigma}_{3i}$, the macro-level spring model for the interface (see, for example, Hashin, 1991) is defined by

$$\overline{k}(\overline{u}_3(\overline{x}_1, 0^+) - \overline{u}_3(\overline{x}_1, 0^-)) = \overline{\sigma}_{32}(\overline{x}_1, 0^+) = \overline{\sigma}_{32}(\overline{x}_1, 0^-), \tag{2}$$

where $\overline{k}$ is the effective stiffness of the interface. Note that $\overline{u}_3(\overline{x}_1, 0^+) - \overline{u}_3(\overline{x}_1, 0^-)$ gives the homogenized displacement jump across the damaged interface.

The conditions in (2) are also given in Benveniste and Miloh (2001). In Benveniste and Miloh (2001), they are derived using an asymptotic analysis on the elastic fields in an infinitesimally thin layer of an extremely soft material bonded between the elastic half-spaces.

To estimate the effective stiffness $\overline{k}$ in the macro-model defined by (2), Wang et al. (2012) simulated the microscopically damaged interface in Fig. 1 by proposing a micromechanical model in which the microscopic voids and defects of the interface are replaced by periodically distributed interfacial micro-cracks. More specifically, the part of the interface defined by $0 < x_1 < L, x_2 = 0$, contains M interfacial micro-cracks with the tips of the mth crack given by $(a^{(m)}, 0)$ and $(b^{(m)}, 0)$, where

$$0 < a^{(1)} < b^{(1)} < a^{(2)} < b^{(2)} < \cdots < a^{(M)} < b^{(M)} < L.$$

The micro-cracks on the remaining part of the interface lie in the regions where $a^{(m)} + nL < x_1 < b^{(m)} + nL$ for $m = 1, 2, \ldots, M$ and $n = \pm 1, \pm 2, \ldots$. The elastic half-spaces are perfectly bonded on the uncracked parts of the interface. The periodically distributed micro-cracks are traction-free under the action of the antiplane constant shear load given by $\sigma_{3i} = \sigma_{3i}^{(\mathrm{int})}$ at infinity, where $\sigma_{3i}^{(\mathrm{int})}$ is the antiplane shear stress in the bimaterial for the corresponding case where there is no micro-crack on the interface. For the studies here, $\sigma_{3i}^{(\mathrm{int})}$ is chosen such that $\sigma_{32}^{(\mathrm{int})} = S_0$ on all the micro-cracks, where S_0 is a positive constant. A sketch of the micromechanical model is given in Fig. 2.

As derived in Wang et al. (2012), the hypersingular integral equations for the micromechanics model of the microscopically damaged interface are given by

$$\begin{aligned}&\sum_{m=1}^{M} \neq\!\!\int_{a^{(m)}}^{b^{(m)}} \Delta u_3(x_1)\left[\frac{1}{x_1-\xi_1} + \frac{1}{(L+x_1-\xi_1)^2} + \frac{1}{(L+\xi_1-x_1)^2}\right.\\ &\left. + \frac{1}{L^2}\psi^*\left(\frac{L+x_1-\xi_1}{L}\right) + \frac{1}{L^2}\psi^*\left(\frac{L+\xi_1-x_1}{L}\right)\right]dx_1\\ &= -\frac{\pi(\beta^{(1)}+\beta^{(2)})}{\beta^{(1)}\beta^{(2)}}S_0 \quad \text{for } a^{(n)} < \xi_1 < b^{(n)} \quad (n = 1, 2, \ldots, M).\end{aligned} \tag{3}$$

where $\neq$ denotes that the integral is to be interpreted in the Hadamard finite-part sense, $\Delta u_3(x_1) = u_3(x_1, 0^+) - u_3(x_1, 0^-)$ denotes the displacement jump across the opposite faces of the micro-cracks, $\psi^*(x) = \psi_1(x) - 1/x^2, \psi_1(x)$ is the trigamma function, $\beta^{(p)} = \sqrt{C_{44}^{(p)}C_{55}^{(p)} - (C_{45}^{(p)})^2}$ and $C_{44}^{(p)}, C_{45}^{(p)}$ and $C_{55}^{(p)}$ are the elastic moduli of the anisotropic materials in the half-spaces ($p = 1$ for the material in $x_2 > 0$ and $p = 2$ for the material in $x_2 < 0$).

A numerical method for solving (3) for the displacement jump $\Delta u_3(x_1)$ over each of the micro-cracks is described in

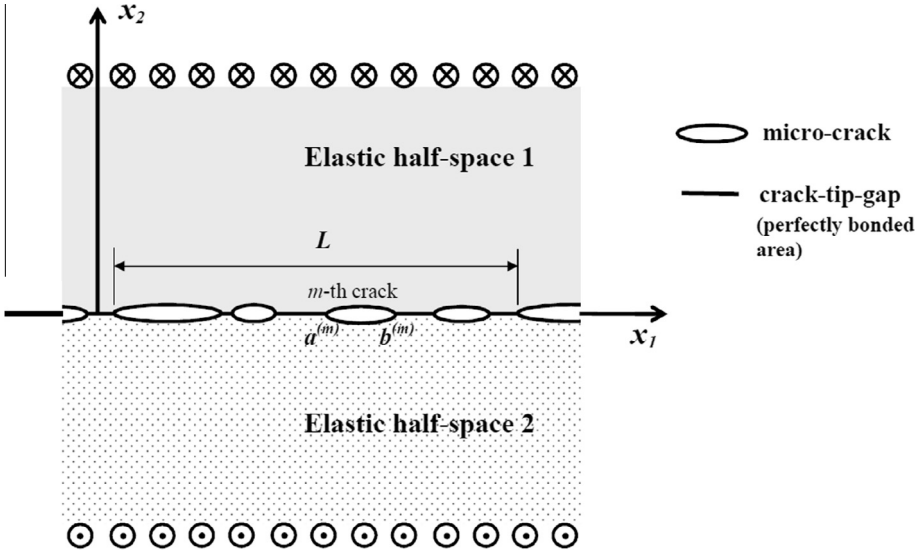

Fig. 2. A sketch of the micromechanical model in Wang et al. (2012).

Wang et al. (2012). The collocation technique of Kaya and Erdogan (1987) may also be used to solve (3) numerically. Once $\Delta u_3(x_1)$ is known over each micro-crack, the effective stiffness $\overline{k}$ of the interface may be estimated using

$$\overline{k} = S_0 L \left[\sum_{m=1}^{M} \int_{a^{(m)}}^{b^{(m)}} \Delta u_3(x_1) dx_1 \right]^{-1}. \tag{4}$$

The mathematics of the micromechanical model used here may be verified numerically as in Wang et al. (2012) by comparing the effective stiffness of a damaged interface containing evenly distributed micro-cracks of equal length with the corresponding effective stiffness predicted by the three-phase model. In Wang et al. (2012), the two models were shown to be in good agreement with each other. For a wide range of values for the crack density on the interface, the percentage difference between the effective stiffness given by the two models is less than 2.5%.

From (4), the effective stiffness of the interface containing M micro-crack per period length may be rewritten as

$$\overline{k} = \frac{\widehat{k}^{(1)} + \widehat{k}^{(2)} + \cdots + \widehat{k}^{(M)}}{M}, \tag{5}$$

where

$$\widehat{k}^{(p)} = \frac{M S_0 L \int_{a^{(p)}}^{b^{(p)}} \Delta u_3(x_1) dx_1}{\left[\sum_{m=1}^{M} \int_{a^{(m)}}^{b^{(m)}} \Delta u_3(x_1) dx_1 \right]^2}, \quad \text{for } p = 1, 2, \ldots, M. \tag{6}$$

For the micromechanical analysis of the macroscopically damaged interface, the length of each micro-crack within a period length of the interface is randomly generated using the probability density function of a chosen statistical distribution. For example, a MATLAB pseudorandom number generator, based on the chi-square distribution, may be used to generate the lengths of the micro-cracks. More details on this are given in Section 3.

The damage ratio denoted by ρ is defined as follows:

$$\rho = \frac{1}{L} \sum_{m=1}^{M} (b^{(m)} - a^{(m)}). \tag{7}$$

Note that ρ gives the fraction of the interface damaged by the interfacial micro-cracks.

3. Statistical simulation

To construct randomly an interface having a given damage ratio ρ, the lengths of M micro-cracks are generated randomly using a statistical distribution. The micro-cracks are then positioned randomly over a period length L. If the average half crack-length of the randomly generated micro-cracks is given by

$$\overline{a} = \frac{1}{2M} \sum_{m=1}^{M} (b^{(m)} - a^{(m)}), \tag{8}$$

then (7) gives rise to the relation $\rho L = 2M\overline{a}$. Note that both sides of the relation denotes the total length of the damaged regions over a period length of the interface. Thus for a fixed damage ratio ρ, the period length L may be calculated easily once the M micro-cracks are randomly generated.

In Wang et al. (2012), the lengths of the micro-cracks are generated randomly using a normal distribution. A more realistic simulation of the statistical distribution of the micro-crack length, based on the chi-squared (χ^2) distribution, is used here. The probability density function of the χ^2 distribution of degree of freedom m is given by

$$f_m(x) = \begin{cases} \frac{x^{-1+m/2} e^{-x/2}}{2^{m/2} \Gamma(m/2)} & \text{for } x \geqslant 0, \\ 0 & \text{for } x < 0, \end{cases} \tag{9}$$

where Γ denotes the gamma function (Abramowitz and Stegun, 1970). Distributions of the lengths of the micro-cracks generated by using the χ^2 distribution of degree of freedom 5, 10 and 25 (denoted by $\chi^2(5), \chi^2(10)$ and $\chi^2(25)$ respectively) are shown visually in Fig. 3. If the χ^2 distribution is of a lower degree of freedom, the distribution of the micro-cracks is more skewed having a greater number of shorter micro-cracks. As the degree of freedom increases, the distribution of the lengths of the micro-cracks becomes less skewed and appears to more normal like.

To form a random sample of N interfaces for statistical analysis, N sets of M micro-cracks are randomly generated and positioned on the interface as described above. For each interface in the sample, the hypersingular integral equations in (3) are solved and the non-dimensionalized interface effective stiffness $\overline{a}(\beta^{(1)} + \beta^{(2)})\overline{k}/(2\beta^{(1)}\beta^{(2)})$ ($\overline{a}$ is the average half-length of the micro-cracks) is calculated using (4). If the values of the non-dimensionalized effective stiffness from the N interfaces are denoted by $y_1, y_2, \ldots, y_{N-1}$ and

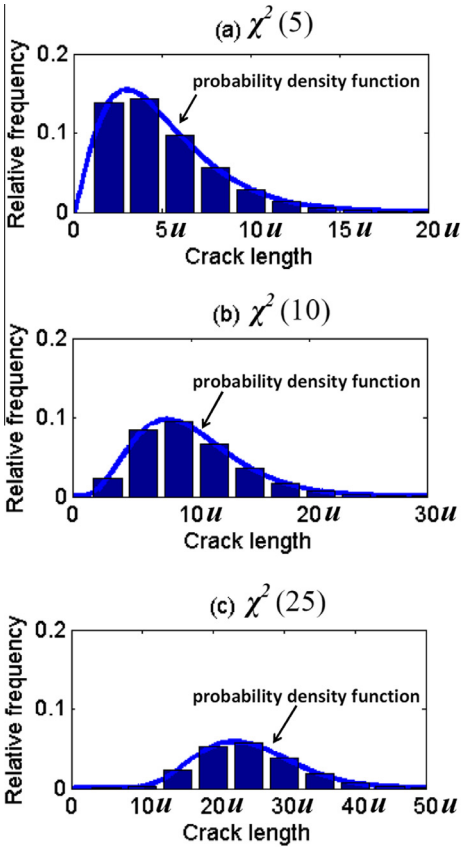

Fig. 3. Distributions of the lengths of micro-cracks generated using $\chi^2(5)$, $\chi^2(10)$ and $\chi^2(25)$. The crack length is in terms of u (a unit length).

y_N, the sample mean of the non-dimensionalized effective stiffness is given by

$$\mu = \frac{1}{N}\sum_{n=1}^{N} y_n \tag{10}$$

and the standard deviation of the N values of the non-dimensionalized effective stiffness from the sample mean μ is

$$s = \sqrt{\frac{1}{N-1}\sum_{n=1}^{N}(y_n-\mu)^2}. \tag{11}$$

The coefficient of variation (CV) defined by

$$\mathrm{CV} = \frac{s}{\mu}\times 100\% \tag{12}$$

is perhaps more useful for analyzing the fluctuation of the statistical data.

4. Number of micro-cracks for homogenizing the interface

To investigate the number of micro-cracks required to homogenize the effective stiffness of the interface in Fig. 2, N interfaces are randomly generated as described in Section 3.

To present some results here, the $\chi^2(5)$ distribution is used to generate the lengths of M micro-cracks on an interface. Table 1 gives the statistical results for the non-dimensionalized effective stiffness $\overline{a}(\beta^{(1)}+\beta^{(2)})\overline{k}/(2\beta^{(1)}\beta^{(2)})$ in a sample of 50 interfaces ($N = 50$) for selected values of the damage ratio ρ. For each value of ρ, it is obvious that the sample mean of the non-dimensionalized stiffness does not change very much as M (the number of micro-cracks per period length) is increased from 40 to 60. Furthermore, the standard deviation (SD) decreases with increasing M. This observation is also demonstrated in Fig. 4 where the variations of the 50 data for the non-dimensionalized stiffness of interfaces with different damage ratios are shown graphically for different numbers of micro-cracks.

Table 1
Statistical results for the non-dimensionalized effective stiffness of the interfaces.

	M	10	20	30	40	60
$\rho = 0.2$	Mean	2.39	2.27	2.07	2.01	2.00
	SD	0.10	0.07	0.07	0.06	0.05
$\rho = 0.4$	Mean	1.11	1.05	0.96	0.92	0.93
	SD	0.05	0.03	0.04	0.03	0.02
$\rho = 0.6$	Mean	0.66	0.63	0.58	0.57	0.56
	SD	0.03	0.02	0.03	0.02	0.02
$\rho = 0.8$	Mean	0.39	0.38	0.36	0.35	0.35
	SD	0.02	0.02	0.01	0.01	0.01

From the results, it appears that around 40 micro-cracks per period length are sufficient to homogenize the effective stiffness of the interface. Further investigations show that the number of micro-cracks required for homogenizing the interface may be lower if a χ^2 distribution of a higher degree of freedom, such as 10 and 25, is used to generate the lengths of the micro-cracks.

For a sample of interfaces with sample size $N = 1000$, the distributions of the 1000 values of the non-dimensionalized effective stiffness of the interfaces with $\rho = 0.2$ are given in Figs. 5 and 6 for $M = 10$ and $M = 40$ respectively. The lengths of the micro-cracks on each interface are generated using the $\chi^2(5)$ distribution. The distribution of the values of the non-dimensionalized effective stiffness for $M = 10$ (a low number of micro-cracks) appears to be skewed to the right. Nevertheless, for $M = 40$, the distribution of the non-dimensionalized stiffness appears to be normal. Similar trends in the distributions are observed when samples of interfaces with other values of the damage ratio ρ are used in the statistical simulations. It appears that 40 micro-cracks over a period length of the interface may be sufficient to homogenize the effective stiffness of the interface.

The statistical simulations above indicate that $\overline{a}(\beta^{(1)}+\beta^{(2)})\overline{k}_{\mathrm{ave}}/(2\beta^{(1)}\beta^{(2)})$ (the average of the non-dimensionalized effective stiffness of all the interfaces in the sample) does not vary much when M (the number of micro-cracks used to simulate an interface) exceed a certain value. Furthermore, the data for the non-dimensionalized effective stiffness $\overline{a}(\beta^{(1)}+\beta^{(2)})\overline{k}/(2\beta^{(1)}\beta^{(2)})$ of the interfaces in the simulation sample appears to be normally distributed for a large value of M. This observation appears to be a direct consequence of the central limit theorem in statistics (Mendenhall et al., 2006), as the formula in (5) for the effective stiffness seems to suggest.

5. Parametric studies on the effective stiffness

The effects of the micro-crack length and the crack-tip gap between two neighboring micro-cracks on the effective stiffness of the interface are examined in the subsections below.

5.1. Effect of the micro-crack length distribution on the effective stiffness

A sample of N interfaces with a given damage ratio ρ is formed. To generate each interface, the lengths of M micro-cracks are

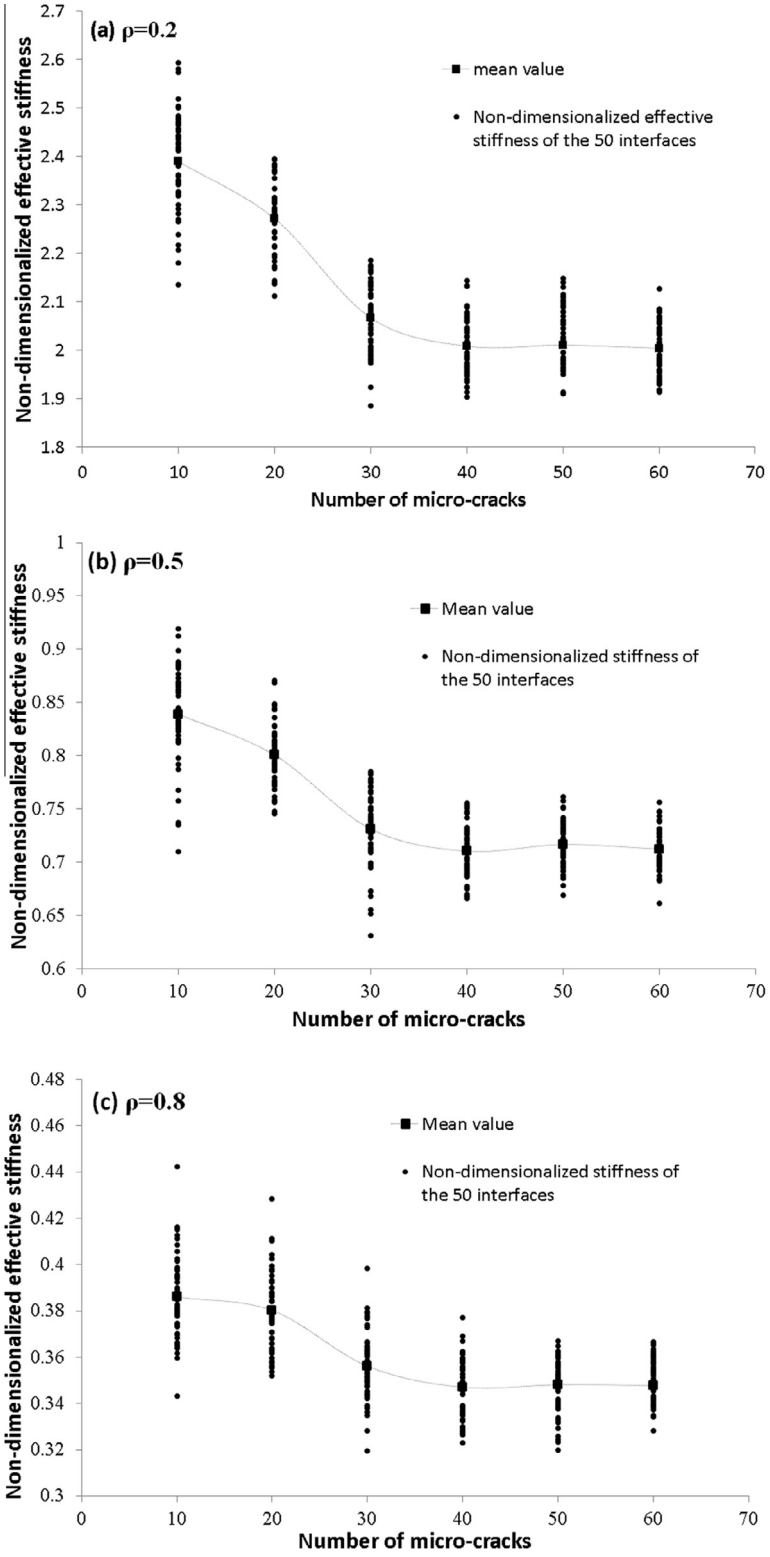

Fig. 4. Scatter plots of the effective stiffness of the interfaces with different damage ratios in samples for different number of micro-cracks. (a) $\rho = 0.2$; (b) $\rho = 0.5$; (c) $\rho = 0.8$.

randomly generated using the $\chi^2(k)$ distribution where k is a fixed positive integer. The micro-cracks are then positioned in such a way that the normalized crack-tip gap length $g/(2\overline{a})$ between any two adjacent micro-cracks is the same given by

$$\frac{g}{2\overline{a}} = \frac{1-\rho}{\rho},$$

where g is the crack-tip gap length before normalization and $\overline{a}$ is the average half length of the M micro-cracks. For fixed ρ, the normalized crack-tip gap length $g/(2\overline{a})$ remains the same for all interfaces within the sample, but the set of lengths of the micro-cracks are different from one interface to another.

The means of $\overline{a}(\beta^{(1)} + \beta^{(2)})\overline{k}/(2\beta^{(1)}\beta^{(2)})$ calculated using a sample of 50 interfaces ($N = 50$) and 40 micro-cracks per period length of

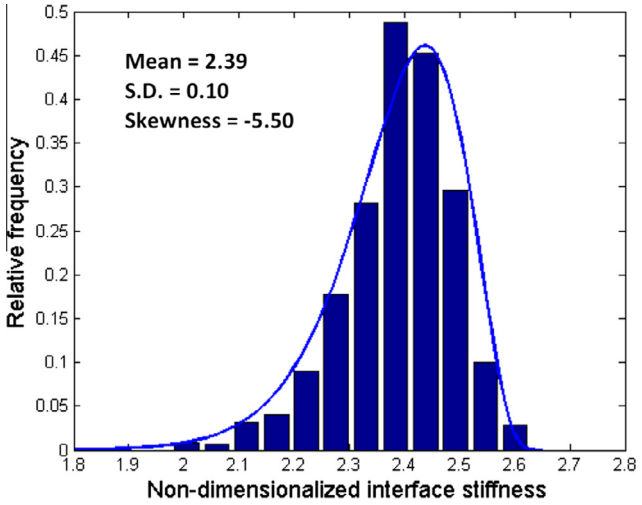

Fig. 5. Distribution of data for the non-dimensionalized effective stiffness of interfaces constructed using 10 micro-cracks per period length.

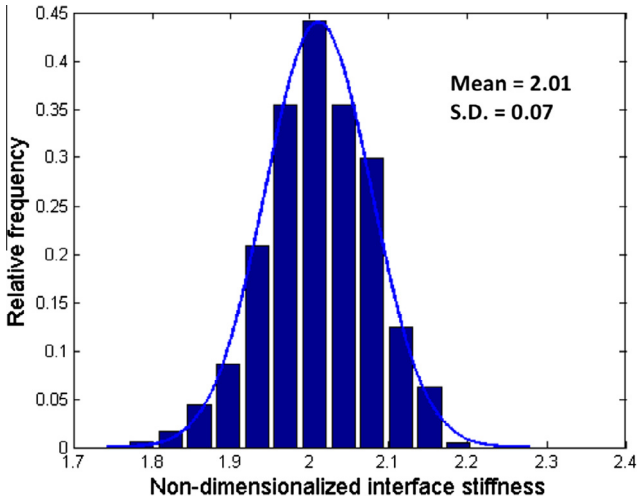

Fig. 6. Distribution of data for the non-dimensionalized effective stiffness of interfaces constructed using 40 micro-cracks per period length.

an interface ($M = 40$) are shown in Table 2 for selected values of the damage ratio ρ and for cases where the lengths of the micro-cracks are generated using χ^2 distributions with degrees of freedom $5, 10$ and 25. For comparison purpose, the corresponding values of the non-dimensionalized effective stiffness calculated using the three-phase model in Wang et al. (2012) are also given in Table 2. The three-phase model is a highly simplified version of the micro-cracked interface in Fig. 2. More details on the three-phase model may be found in the Appendix A.

From Table 2, for a fixed ρ, the mean is closer to the non-dimensionalized effective stiffness calculated using the three-phase model as the degree of freedom of the χ^2 distribution used becomes larger, that is, as the distribution of the micro-crack length becomes more normal like. This is as expected, as the three-phase model assumes that the micro-cracks are of equal length and are evenly distributed on the interface. Also, for a χ^2 distribution of a lower degree of freedom, the mean of the non-dimensionalized stiffness appears to be smaller, while the standard deviation is larger. Perhaps this observation on the mean may be explained by taking into consideration that most of the micro-cracks tend to be short and the ratio of the length of the longest micro-crack to that of the shortest micro-crack is relatively large if the χ^2 distribution used is of a lower degree of freedom. For example, the ratio is likely around 1000 for the $\chi^2(5)$ distribution, but it is likely around 3 for the $\chi^2(25)$ distribution.

The non-dimensionalized mean effective stiffness in Table 2 is plotted against the damage ratio ρ in Fig. 7 for the χ^2 distributions of degrees of freedom $5, 10$ and 25 as well as for the three-phase model. The effect of the degree of freedom of the χ^2 distribution on the non-dimensionalized effective stiffness as discussed above is clearly shown in Fig. 7.

5.2. Effect of the micro-crack tip gap distribution on the effective stiffness

A sample of N interfaces with a fixed damage ratio ρ is generated by placing M equal length micro-cracks over a period length L of the interface. The micro-crack tip gap g between any two consecutive neighboring micro-cracks is generated randomly using the $\chi^2(k)$ distribution. The mean of g, denoted by $\overline{g}$, is related to micro-crack half length a by

$$\frac{2a}{\overline{g}} = \frac{\rho}{1-\rho}.$$

The means of $\overline{a}(\beta^{(1)} + \beta^{(2)})\overline{k}/(2\beta^{(1)}\beta^{(2)})$ calculated using $N = 50$ and $M = 40$ are shown in Table 3 for selected values of the damage ratio ρ and for micro-crack tip gaps generated using χ^2 distributions with degrees of freedom $5, 10$ and 25. The corresponding values of the non-dimensionalized effective stiffness calculated using the three-phase model in Wang et al. (2012) are also given in Table 3. It is obvious that the mean in Table 3 for a fixed value of ρ is smaller if χ^2 distribution used is of a lower degree of freedom. This may be explained by taking into consideration that the χ^2 distribution of a lower degree of freedom generates micro-crack tip gaps that skew towards having shorter lengths, giving rise to Δu_3 of a higher magnitude on most of the micro-cracks. Nevertheless, the graphs of the non-dimensionalized effective stiffness against

Table 2
The mean, standard deviation (SD) and coefficient of variation (CV (%)) of the non-dimensionalized effective stiffness for selected values of the damage ratio ρ and for distributions of micro-crack length generated using the $\chi^2(5), \chi^2(10)$ and $\chi^2(25)$ distributions.

ρ	$\chi^2(5)$			$\chi^2(10)$			$\chi^2(25)$			Three-phase model
	Mean	SD	CV(%)	Mean	SD	CV(%)	Mean	SD	CV(%)	
0.1	4.255	0.114	2.672	5.381	0.047	0.874	5.998	0.012	0.194	6.335
0.2	2.096	0.056	2.673	2.654	0.023	0.870	2.961	0.006	0.196	3.120
0.3	1.366	0.036	2.650	1.731	0.016	0.905	1.931	0.004	0.206	2.029
0.4	0.991	0.027	2.703	1.257	0.012	0.959	1.402	0.003	0.229	1.467
0.5	0.760	0.022	2.927	0.963	0.009	0.962	1.072	0.002	0.199	1.118
0.6	0.597	0.016	2.708	0.755	0.007	0.941	0.840	0.002	0.260	0.873
0.7	0.473	0.014	2.968	0.596	0.006	1.041	0.661	0.002	0.288	0.686
0.8	0.369	0.010	2.771	0.462	0.005	1.060	0.511	0.001	0.267	0.532
0.9	0.273	0.008	3.043	0.335	0.003	0.984	0.366	0.001	0.280	0.388

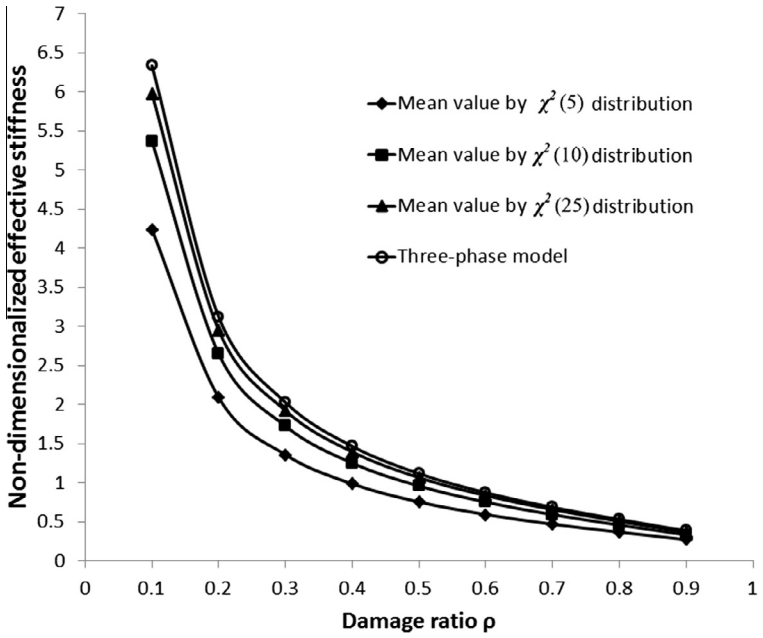

Fig. 7. Plots of non-dimensionalized effective stiffness against the damage ratio ρ, for distributions of micro-crack length generated using the $\chi^2(5), \chi^2(10)$ and $\chi^2(25)$ distributions. Also included are the corresponding values predicted by the three-phase model.

Table 3
The mean, standard deviation (SD) and coefficient of variation (CV (%)) of the non-dimensionalized effective stiffness for selected values of the damage ratio ρ and for distributions of micro-crack tip gap generated using the $\chi^2(5), \chi^2(10)$ and $\chi^2(25)$ distributions.

ρ	$\chi^2(5)$			$\chi^2(10)$			$\chi^2(25)$			Three-phase model
	Mean	SD	CV(%)	Mean	SD	CV(%)	Mean	SD	CV(%)	
0.1	6.209	0.015	0.236	6.327	0.001	0.021	6.336	0.0004	0.007	6.335
0.2	3.009	0.013	0.419	3.110	0.001	0.046	3.124	0.001	0.022	3.120
0.3	1.933	0.010	0.515	2.019	0.002	0.106	2.034	0.001	0.036	2.029
0.4	1.382	0.008	0.558	1.459	0.002	0.156	1.475	0.001	0.059	1.467
0.5	1.045	0.005	0.478	1.111	0.002	0.163	1.125	0.001	0.062	1.118
0.6	0.813	0.004	0.435	0.867	0.002	0.181	0.880	0.001	0.097	0.873
0.7	0.637	0.005	0.713	0.679	0.001	0.211	0.690	0.001	0.119	0.686
0.8	0.490	0.003	0.634	0.522	0.001	0.248	0.531	0.001	0.113	0.532
0.9	0.353	0.002	0.562	0.373	0.001	0.217	0.379	0.001	0.132	0.388

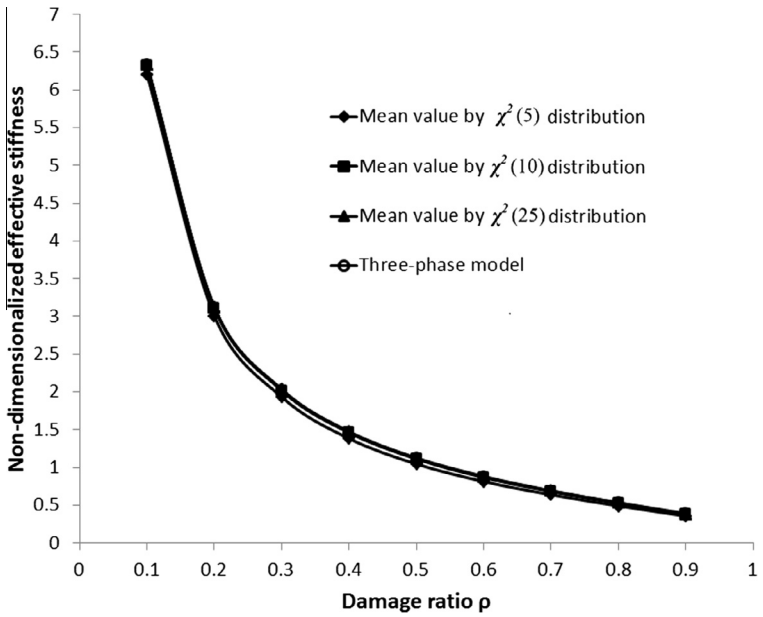

Fig. 8. Plots of non-dimensionalised mean effective stiffness against the damage ratio ρ, for distributions of micro-crack tip gap generated using the $\chi^2(5), \chi^2(10)$ and $\chi^2(25)$ distributions. Also included are the corresponding values predicted by the three-phase model.

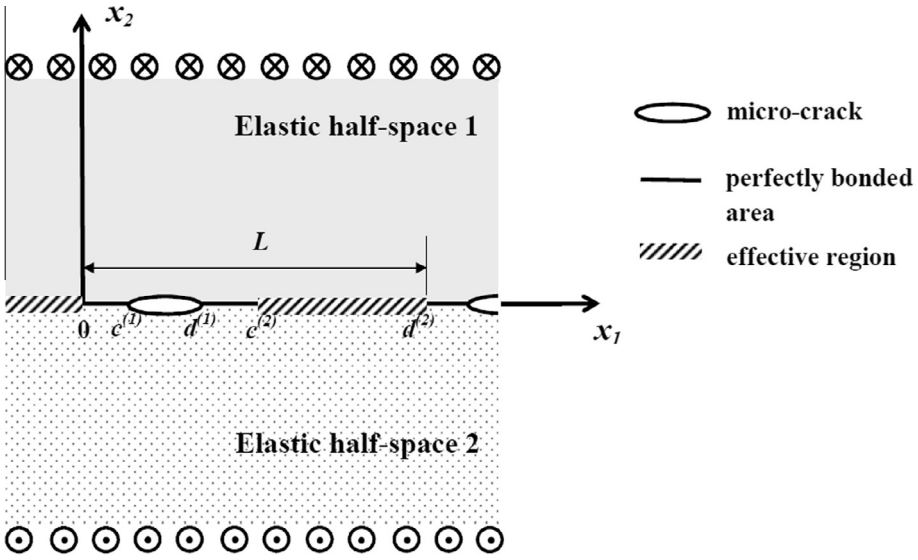

Fig. 9. A sketch of the three-phase model.

the damage ratio ρ do not show much difference in Fig. 8 for the $\chi^2(5), \chi^2(10)$ and $\chi^2(25)$ distributions compared to the graphs in Fig. 7. It seems that varying the distribution of the micro-crack tip gaps does not affect the mean effective stiffness as much as varying the distribution of the lengths of the micro-cracks.

It is also seen that the standard deviation of non-dimensionalized effective stiffness listed in Table 2 is obviously larger than the corresponding standard deviation in Table 3. Similarly, the CVs of $\overline{a}(\beta^{(1)}+\beta^{(2)})\overline{k}/(2\beta^{(1)}\beta^{(2)})$ in Table 2 are larger than the corresponding ones in Table 3. This seems to suggest that the variation of the micro-crack lengths has a greater influence on the scattering of the non-dimensionalized effective stiffness than the variation of the micro-crack tip gaps. This observation is consistent with our understanding that lengths of the micro-cracks directly affect the displacement jumps over the micro-cracks, while the gap between micro-cracks does not affect the displacement jump as significantly as crack-lengths. Note that the effective stiffness of the interface is calculated by averaging the displacement jumps.

6. Summary and conclusions

Prior to the micromechanical-statistical simulations in Wang et al. (2012), the three-phase model was the only micromechanical model estimating the effective stiffness (see Fan and Sze, 2001). The only parameter used in the three-phase model is the damage ratio (crack density) ρ. In estimating the effective stiffness, the statistical simulations in Wang et al. (2012) takes into consideration more microscopic details, such as statistical variations of the lengths of the interfacial micro-cracks. Nevertheless, in Wang et al. (2012), the micro-crack lengths are assumed to vary according to a normal distribution. This may not depict accurately the realistic situation where the statistical distribution of the micro-crack lengths tends to be skewed towards shorter micro-cracks.

In the present paper, microscopically damaged interfaces between two anisotropic elastic half-spaces under antiplane loads are modeled as interfaces containing periodically distributed micro-cracks. The micro-cracked interfaces are simulated statistically to calculate the interface effective stiffness. For more realistic simulations, the χ^2 distribution is used to generate randomly the lengths of the micro-cracks.

Statistical simulations conducted suggest that around 40 or more micro-cracks per period length of the interface are required to homogenize the interface effective stiffness. If interfaces are statistically simulated using a sufficient number of micro-cracks, the data of the appropriately non-dimensionalized effective stiffness can be fitted into a normal distribution.

The crack length distribution is to be provided by experimental observation. For a highly skewed crack-length distribution such as $\chi^2(5)$, the effective stiffness by statistical simulation may be 30% lower than that predicted by the three-phase model in Wang et al. (2012). If the micro-crack length is generated using a less skewed χ^2 distribution such as $\chi^2(25)$, the mean effective stiffness is found to agree with that given by the three-phase model to within 6% for a wide range of the damage ratio ρ of the interface. Furthermore, the distribution of the micro-crack length appears to have a stronger influence on mean and standard deviation of the effective stiffness than the distribution of the micro-crack tip gaps. The non-dimensionalized effective stiffness in a sample of interfaces generated using micro-cracks of varying lengths and equal length micro-crack tip gaps deviates more from the mean value than the non-dimensionalized effective stiffness in a corresponding sample of interfaces generated using equal length micro-cracks with varying micro-crack tip gaps.

Appendix A

A highly simplified version of the micro-cracked interface in Fig. 2 is the three-phase model given in Wang et al. (2012). The interface is still periodic in the three-phase model, but a period length of the interface, denoted by $0 < x_1 < L, x_2 = 0$, is divided into three distinct types of regions described as follows:

(a) a single representative micro-crack $c^{(1)} < x_1 < d^{(1)}, x_2 = 0$,
(b) perfectly bonded parts defined by $0 < x_1 < c^{(1)}$ and $d^{(1)} < x_1 < c^{(2)}$ on $x_2 = 0$, and
(c) an effective region $c^{(2)} < x_1 < d^{(2)}, x_2 = 0$, where the constants $c^{(1)}, c^{(2)}, d^{(1)}$ and $d^{(2)}$ are such that $0 < c^{(1)} < d^{(1)} < c^{(2)} < d^{(2)} = L, c^{(1)} = c^{(2)} - d^{(1)}$ and $c^{(2)}$ is much smaller than L.

A sketch of the three-phase model is given in Fig. 9.

For the three phase model here, the damage ratio ρ which corresponds to (7) is defined by

$$\rho = \frac{d^{(1)} - c^{(1)}}{c^{(2)}}.$$

As derived in Wang et al. (2012), the hypersingular integral equations for the three-phase model are given by

$$\sum_{i=1}^{2} \oint_{c^{(i)}}^{d^{(i)}} \Delta u_3(x_1) \left[\frac{1}{(x-\xi_1)^2} + \frac{1}{(d^{(2)}+x_1-\xi_1)^2} + \frac{1}{(d^{(2)}+\xi_1-x_1)^2} + \frac{1}{[d^{(2)}]^2}\psi^*\left(\frac{d^{(2)}+x_1-\xi_1}{d^{(2)}}\right) + \frac{1}{[d^{(2)}]^2}\psi^*\left(\frac{d^{(2)}+\xi_1-x_1}{d^{(2)}}\right)\right] dx_1 = -\frac{\pi(\beta^{(1)}+\beta^{(2)})}{\beta^{(1)}\beta^{(2)}} \begin{cases} S_0 & \text{for } c^{(1)} < \xi_1 < d^{(1)}, \\ S_0 - \bar{k}\Delta u_3(\xi_1) & \text{for } c^{(2)} < \xi_1 < d^{(2)}, \end{cases} \tag{A1}$$

where Δu_3 denotes the jump of u_3 across opposite faces of the micro-cracks and the effective regions, S_0 is a positive constant relating to the internal antiplane constant shear load acting on the micro-cracks and $\bar{k}$ is the effective stiffness to be determined.

As the effective stiffness $\bar{k}$ is a macroscopic quantity that is not known a priori, an iterative procedure may be used to solve the hypersingular integral equations in (A1) together with

$$\frac{\bar{k}}{c^{(2)}} \int_{c^{(1)}}^{d^{(1)}} \Delta u_3(x_1) dx_1 = S_0. \tag{A2}$$

References

Aboudi, J., 1991. Mechanics of Composite Materials: A Unified Micromechanical Approach. Elsevier, New York.

Abramowitz, M., Stegun, I., 1970. Handbook of Mathematical Functions. Dover, New York.

Ang, W.T., 2007. Elastodynamic antiplane deformation of a bimaterial with an imperfect viscoelastic interface: a dual reciprocity hypersingular boundary integral solution. Appl. Math. Modell. 31, 749–769.

Ang, W.T., 2013. Hypersingular Integral Equations in Fracture Analysis. Woodhead Publishing, Cambridge.

Benveniste, Y., Miloh, T., 2001. Imperfect soft and stiff interfaces in two-dimensional elasticity. Mech. Mater. 33, 309–323.

Christensen, R.M., 1990. A critical evaluation for a class of micromechanics models. J. Mech. Phys. Solids 38, 379–404.

Elvin, A.A., 1996. Number of grains required to homogenize elastic properties of polycrystalline ice. Mech. Mater. 22, 51–64.

Fan, H., Sze, K.Y., 2001. A micro-mechanics model for imperfect interface in dielectric materials. Mech. Mater. 33, 363–370.

Fan, H., Wang, G.F., 2003. Interaction between a screw dislocation and viscoelastic interfaces. Int. J. Solids Struct. 40, 763–776.

Hamidi, Y.K., Aktas, L., Altan, M.C., 2004. Formation of microscopic voids in resin transfer molded composites. J. Eng. Mater. Technol. 126, 420–426.

Hashin, Z., 1991. The spherical inclusion with imperfect interface. ASME J. Appl. Mech. 58, 444–449.

Jones, J.P., Whittier, J.S., 1967. Waves at a flexibly bonded interface. J. Appl. Mech. 34, 905–909.

Kaya, A.C., Erdogan, F., 1987. On the solution of integral equations with strongly singular kernels. Q. Appl. Math. 45, 105–122.

Li, S., Wang, G., 2008. Introduction to Micromechanics and Nanomechanics. World Scientific Pub Co Inc, Hackensack, NJ.

Margetan, F.J., Thompson, R.B., Gray, T.A., 1988. Interfacial spring model for ultrasonic interactions with imperfect interfaces. J. Nondestr. Eval. 7, 131–152.

Mendenhall, W., Beaver, R.J., Beaver, B.M., 2006. Introduction to Probability and Statistics. Thomson, Singapore.

Nix, W.D., 1989. Mechanical properties of thin films. Metall. Trans. A 20, 2217–2245.

Roberts, A.P., Garboczi, E.J., 1999. Elastic properties of a tungsten-silver composite by reconstruction and computation. J. Mech. Phys. Solids 47, 2029–2055.

Torquato, S., 2002. Statistical description of microstructures. Ann. Rev. Mater. Res. 32, 71–111.

Wang, X., Ang, W.T., Fan, H., 2012. Micro-mechanics models for an imperfect interface under anti-plane shear load: hypersingular integral formulations. Eng. Anal. Boundary Elem. 36, 1856–1864.

Zhong, Z., Meguid, S.A., 1997. On the elastic field of a spherical inhomogeneity with an imperfectly bonded interface. J. Elast. 46, 91–113.